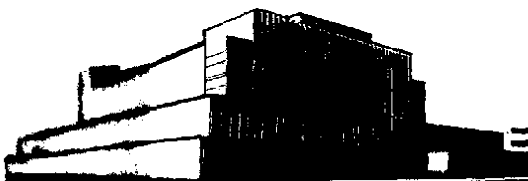


# STRENGTH OF ORTHOTROPIC MATERIALS SUBJECTED TO COMBINED STRESSES

Information Reviewed and Reaffirmed

May 1962

No. 1816



FOREST PRODUCTS LABORATORY  
MADISON · WISCONSIN

UNITED STATES DEPARTMENT OF AGRICULTURE  
FOREST SERVICE

In Cooperation with the University of Wisconsin

# STRENGTH OF ORTHOTROPIC MATERIALS SUBJECTED TO COMBINED STRESSES<sup>1</sup>

By

CHARLES B. NORRIS, Engineer

Forest Products Laboratory,<sup>2</sup> Forest Service  
U.S. Department of Agriculture

---

## Summary

A theory of the strength of orthotropic materials subjected to combined stresses, based on the Henky-vonMises theory of energy due to change of shape, is presented. When this theory is applied to macroscopically isotropic materials, it yields the diagram currently used in design with metals. Equations relating the strength of orthotropic materials subjected to a single stress at angles to the natural axes of the material are deduced from the theory. These equations are shown to agree with available test values.

## Introduction

The most common orthotropic material (that is, a material which has different mechanical properties in the directions of three mutually perpendicular axes-- called the natural axes) is wood. Plywood can be considered to be orthotropic under certain conditions. Paper and paper laminates are also orthotropic. Resin laminates made of sheets of woven glass fiber, as used in radomes of aircraft, are also orthotropic, as are most of the core materials used in sandwich panels in the construction of high-speed aircraft.

To obtain rational designs of structures made of these materials, it is necessary to have knowledge concerning their strength when they are subjected to combined stresses. Further, if they are subjected to a single stress at angles to their natural axes, this stress is resolved into components associated with the natural axes and acts as a set of combined stresses. This fact was pointed out by

---

<sup>1</sup>This report is one of a series prepared and distributed by the Forest Products Laboratory under U.S. Navy, Bureau of Aeronautics Order No. NBA-PO-NAer00854 and USAF-PO-(33-038)49-4696E. Results here reported were obtained during 1950.

<sup>2</sup>Maintained at Madison, Wis., in cooperation with the University of Wisconsin.

C. F. Jenkins (7)<sup>3</sup> in 1920. He suggested that when an orthotropic material is loaded by a single stress the stress is resolved into the stresses associated with the natural axes, and that the strength of the material is reached when any one of these resolved stresses reaches its maximum value, as determined by tests in which that component of the single stress is applied alone. This method was overlooked by previous investigators (5,6) in the field.

In 1920, a number of investigators (2,4,10,21) became interested in the compressive strength of wood at an angle to the direction of the grain. During this same time, tests were being carried out by the Material Section of the Air Service under the direction of R. L. Hankinson (26). These tests led to an empirical formula known as the Hankinson formula, which is now in general use.

The Hankinson formula does not contain the shear strength of the wood but merely the compressive strengths parallel and perpendicular to the grain of the wood. The compressive strength perpendicular to the grain is difficult to determine because, as the load is increased, the wood will crush down and the load will increase indefinitely, reaching a value of about 10,000 pounds per square inch when the volume of the wood is reduced to about one-half its original volume. R. C. Rowse (20) avoided this difficulty by applying the Hankinson formula to proportional limit stresses rather than to strengths. He found that the Hankinson formula fitted his experimental data reasonably well.

In 1928, W. R. Osgood (19) analyzed much of the available experimental data and pointed out that if a formula is fitted to this data it should contain a means of adjusting the strength in the neighborhood of 45°. He suggested an empirical formula that made such adjustment possible.

The author (13) roughly applied the Henky-vonMises theory (11,12) of constant energy due to change of shape to wood, and pointed out that the Hankinson formula tacitly assumes a relation between the shear strength (associated with the natural axes) and the two compressive strengths.

During the Second World War, this matter again became important in connection with the use of plywood and other orthotropic materials in aircraft construction. The author (15) suggested the use of an interaction formula, which again brought in the influence of the shear strength associated with the natural axes of the material. This empirical formula fitted the experimental data so well that it seemed to point to some existing physical mechanism responsible for the strength of orthotropic materials. Its form suggested the Henky-vonMises theory.

In the present report, a theory for the strength of orthotropic materials, based upon the Henky-vonMises theory for isotropic materials, is developed by a method that is not rigorously correct. The orthotropic materials are assumed to be made from an isotropic material by introducing regularly spaced voids. The formula obtained is identical to the interaction formula except

---

<sup>3</sup>Underlined numbers in parentheses refer to literature cited at the end of this report.

for an added term that has a low value in the range in which tests have been made. The formula can be reduced to apply to isotropic materials having heterogeneously distributed voids, and when so reduced it leads to the criterion for failure of metals that is currently in use. The results of tests on wood, plywood, and fiberglass laminate are compared with values obtained by means of the formula, and good agreement is found.

### Mathematical Development

#### The General Henky-vonMises Theory

Consider an isotropic material subjected to a stress system. A unit cube within the material oriented with respect to an arbitrarily chosen set of orthogonal axes, 1, 2, and 3, is shown in figure 1. These axes are not principal axes of stress and, therefore, the surfaces of the cube are subject to shear stresses as well as direct stresses, as shown. The energy of deformation of this cube is determined by replacing the strains by the stresses by use of Hooke's law for elastic deformation.

$$\begin{aligned}
 E\epsilon_1 &= s_1 - v(s_2 + s_3) \\
 E\epsilon_2 &= s_2 - v(s_3 + s_1) \\
 E\epsilon_3 &= s_3 - v(s_1 + s_2) \\
 G\epsilon_{12} &= s_{12} \\
 G\epsilon_{23} &= s_{23} \\
 G\epsilon_{31} &= s_{31}
 \end{aligned}
 \tag{1}$$

$E$  = modulus of elasticity

$G$  = modulus of rigidity

$s$  = stress. The subscripts denote directions. Single subscripts denote direct stresses, and double subscripts denote shear stresses.

$e$  = strain. The subscripts denote directions as for stresses.

$v$  = Poisson's ratio

Using these equations the total energy of deformation is:

$$W = \frac{1}{2E} \left[ s_1^2 + s_2^2 + s_3^2 - 2v(s_1s_2 + s_2s_3 + s_3s_1) \right] + \frac{1}{2G} \left[ s_{12}^2 + s_{23}^2 + s_{31}^2 \right] \quad (2)$$

The energy of change of volume is:

$$W_v = \frac{1}{6} (s_1 + s_2 + s_3) (\epsilon_1 + \epsilon_2 + \epsilon_3) = \frac{1}{6E} (1 - 2v) (s_1 + s_2 + s_3)^2 \quad (3)$$

The energy of the shear strains does not appear in this equation, because shear strains do not change the volume. The energy of change of shape is  $W_s = W - W_v$  or:

$$W_s = \frac{1}{12G} \left[ (s_1 - s_2)^2 + (s_2 - s_3)^2 + (s_3 - s_1)^2 \right] + \frac{1}{2G} \left[ s_{12}^2 + s_{23}^2 + s_{31}^2 \right] \quad (4)$$

The Henky-vonMises theory assumes that the energy,  $W_s$ , has a definite value when the proportional limit of the material is reached, no matter what combination of stresses is applied to the material. If stress  $s_1$  is applied alone and given the proportional limit value,  $p$ , equation (4) yields:

$$W_s = \frac{p^2}{6G}$$

By using this value, equation (4) becomes:

$$p^2 = \frac{1}{2} \left[ (s_1 - s_2)^2 + (s_2 - s_3)^2 + (s_3 - s_1)^2 \right] + 3 \left[ s_{12}^2 + s_{23}^2 + s_{31}^2 \right] \quad (4a)$$

This equation can be applied at failure for some materials. The octahedral shear stress-strain curve (11,12) of such a material is given in figure 2, with the proportional limit occurring at point A and failure at point B. Suppose the material is to be loaded just short-offailure and the stress then released. The stress-strain curve during release of the stress is like BC.

On reloading, CB becomes the stress-strain curve, which is a straight line to failure. Thus the material, treated in this way, acts elastically to failure during the second loading. The condition of the material when point B is reached is the same whether the release of stress and the reloading to that point take place or not. The energy involved,  $\underline{W}_S$ , can be considered to be that associated with the reloading. For the material in this condition, the proportional limit stress is equal to the stress at failure, and thus equation (4a) will apply at failure for such a material. Many materials act substantially in this way (11,12,27,29).

#### The Formula for Orthotropic Materials

Now consider an orthotropic material made up of an isotropic material by introducing voids in the shape of equal rectangular prisms. The walls of isotropic material between these voids are parallel to the 1-2, 2-3, and 3-1 planes, so that the axes 1, 2, and 3 become the natural axes of the orthotropic material.

Each set of walls is subjected to a two-dimensional stress system, since the surfaces of the walls are free from stress. Thus three equations for energy due to change of shape are obtained, one for each set of walls. These equations are obtained from equation (4). Thus:

$$\begin{aligned} W_S &= \frac{1}{6G} \left[ s_1^2 - s_1 s_2 + s_2^2 \right] + \frac{1}{2G} s_{12}^2 \\ W_S &= \frac{1}{6G} \left[ s_2^2 - s_2 s_3 + s_3^2 \right] + \frac{1}{2G} s_{23}^2 \\ W_S &= \frac{1}{6G} \left[ s_3^2 - s_3 s_1 + s_1^2 \right] + \frac{1}{2G} s_{31}^2 \end{aligned} \quad (5)$$

If it be assumed, for the moment, that the walls between the voids do not buckle when they are stressed, the values of the stresses,  $\underline{s}$ , in the isotropic walls will be proportional to the values of the gross stresses,  $\underline{f}$ , applied to the orthotropic material because of the geometry of the material. These proportionalities are expressed by:

$$\begin{aligned} s_1 &= r_1 f_1 & s_{12} &= r_{12} f_{12} \\ s_2 &= r_2 f_2 & s_{23} &= r_{23} f_{23} \\ s_3 &= r_3 f_3 & s_{31} &= r_{31} f_{31} \end{aligned} \quad (6)$$

When a shear stress, say  $\underline{f_{12}}$ , is applied alone, the set of walls parallel to the 1 and 2 plane are subjected to edgewise shear. The two sets of walls perpendicular to these walls are also subjected to shear in the 1 and 2 plane where they are joined to the first set of walls (fig. 3). Thus the reaction of the orthotropic material to the shear stress is greater than that of the first set of walls acting alone. This fact is taken into account in the value of the ratio  $\underline{r_{12}}$ . Further, the second two sets of walls are subjected to some bending. The effect of this bending is neglected.

Substituting the values given by equation (6) in equation (5):

$$\begin{aligned} W_s &= \frac{1}{6G} \left[ r_1^2 f_1^2 - r_1 f_1 r_2 f_2 + r_2^2 f_2^2 \right] + \frac{1}{2G} r_{12}^2 f_{12}^2 \\ W_s &= \frac{1}{6G} \left[ r_2^2 f_2^2 - r_2 f_2 r_3 f_3 + r_3^2 f_3^2 \right] + \frac{1}{2G} r_{23}^2 f_{23}^2 \\ W_s &= \frac{1}{6G} \left[ r_3^2 f_3^2 - r_3 f_3 r_1 f_1 + r_1^2 f_1^2 \right] + \frac{1}{2G} r_{31}^2 f_{31}^2 \end{aligned} \quad (7)$$

Now assume that the energy  $\underline{W_s}$  has just the value associated with failure of the isotropic material. First let all the stresses but  $\underline{f_1}$  be zero; then

$$W_s = \frac{1}{6G} r_1^2 F_1^2$$

in which  $\underline{F_1}$  denotes the stress at failure obtained from test under this condition. Solving this equation for  $\underline{r_1}$

$$r_1 = \frac{\sqrt{6 G W_s}}{F_1}$$

Repeating this procedure for the other stresses, the following equations are obtained:

$$\begin{aligned} r_2 &= \frac{\sqrt{6 G W_s}}{F_2} \\ r_3 &= \frac{\sqrt{6 G W_s}}{F_3} \end{aligned}$$

$$r_{12} = \frac{\sqrt{2GW_s}}{F_{12}}$$

$$r_{23} = \frac{\sqrt{2GW_s}}{F_{23}}$$

$$r_{31} = \frac{\sqrt{2GW_s}}{F_{31}}$$

When these values are substituted in equation (7), the following equations result:

$$\begin{aligned} 1 &= \frac{f_1^2}{F_1^2} - \frac{f_1 f_2}{F_1 F_2} + \frac{f_2^2}{F_2^2} + \frac{f_{12}^2}{F_{12}^2} \\ 1 &= \frac{f_2^2}{F_2^2} - \frac{f_2 f_3}{F_2 F_3} + \frac{f_3^2}{F_3^2} + \frac{f_{23}^2}{F_{23}^2} \\ 1 &= \frac{f_3^2}{F_3^2} - \frac{f_3 f_1}{F_3 F_1} + \frac{f_1^2}{F_1^2} + \frac{f_{31}^2}{F_{31}^2} \end{aligned} \quad (8)$$

Cellular orthotropic materials often exhibit strengths in compression of lesser values than those exhibited in tension. This phenomenon is attributed to the buckling of the walls between the voids when they are subjected to a compressive stress. Figure 3 is a sketch of a single wall with some of the surrounding material still attached. The wall is buckled by the stresses  $s_1$  and  $s_2$ . This buckling takes place because the edges of the wall are shortened by these stresses. The buckled surface is shown by the dotted lines CAB and DAE, which fell on the dash-dot lines COB and DOE before buckling took place. The corners of the wall, E, remain substantially flat even after buckling occurs.

The maximum load the wall will carry is attained when the material at the edges of the wall fails. Failure will occur at the corners of the wall, for here the material is subjected to the combined effect of stresses  $s_1$  and  $s_2$ . At the centers of the edges, at C or E, the effect of one of the stresses is reduced because of the buckling of the wall. Failure may take place in these regions because of combined compression and bending, but the maximum load on the wall as a whole will not be reached until the material at the corners fails. The addition of edgewise shear stresses to the wall does not greatly alter this situation.



When the balls buckle, the values of the ratios,  $\underline{r}$ , do not remain constant as the mean stresses,  $\underline{f}$ , are increased, however; for any particular orthotropic material, there are definite values of these ratios associated with the maximum loads the walls will carry, and thus associated with the maximum values of the mean stresses,  $\underline{F}$ . When the stress  $\underline{s}_1$  is applied alone, it can be assumed (25) that the load on the plate is carried by two uniformly loaded strips at the edges of the plate, each of width  $\underline{c}_1$  as shown in figure 3. The width of these strips decreases as the stress is increased and has a definite value at the maximum load. The width of the strips is given by:

$$\underline{c}_1 = \pi h \sqrt{\frac{E}{12s_1(1 - \nu^2)}}$$

in which  $\underline{h}$  is the thickness of the wall. In figure 4, the radical is plotted against the ratio of the stress to the modulus of elasticity. It is evident that at high stresses the width of the strips does not change rapidly with the stress. It will be assumed that  $\underline{c}_1$  remains substantially constant in this range. When the stresses  $\underline{s}_1$  and  $\underline{s}_2$  are applied together, equation (4a) indicates that at failure the magnitude of one of them is in this range and will control failure. The addition of a shear stress will not greatly alter this situation, because shear stresses are effected only slightly by buckling.

It follows that equations (8) apply with reasonable accuracy to cellular orthotropic materials, even when the walls buckle before the maximum load is reached. It should be noted, however, that the value of  $\underline{F}_1$ ,  $\underline{F}_2$ , or  $\underline{F}_3$  may be different when the mean stress  $\underline{f}_1$ ,  $\underline{f}_2$ , or  $\underline{f}_3$  is compressive rather than tensile,.. When a mean stress is tensile, the tensile value of the associated  $\underline{E}$  should be used; and when it is compressive, the compressive value of the associated  $\underline{E}$  should be used.

Each of equations (8) represents an ellipsoid with its center at the origin. These ellipsoids occupy a six-dimensional space. Any condition of stress is represented by a point in this space. If the point lies within the volume common to all three ellipsoids, the material will not fail. As the stresses increase, the point representing them moves outward from the origin, and when it reaches the surface of any one of these ellipsoids, the orthotropic material will fail.

Plane stress.--It is difficult to visualize these three ellipsoids in six-dimensional space. However, only three dimensions of this space are needed if the stress system applied to the orthotropic material is limited to one of the natural planes. If the plane 1-2 is chosen,  $\underline{f}_3 = \underline{f}_{23} = \underline{f}_{31} = 0$ , and equations (8) reduce to:

$$1 = \frac{f_1^2}{F_1^2} - \frac{f_1 f_2}{F_1 F_2} + \frac{f_2^2}{F_2^2} + \frac{f_{12}^2}{F_{12}^2}$$

$$\frac{f_2^2}{F_2^2} = 1 \quad (9)$$

$$\frac{f_1^2}{F_1^2} = 1$$

These equations define an ellipsoid and four planes in three-dimensional space. Two octants of the figure are shown in figure 5. The three parameters

represented in this figure are  $\frac{f_1}{F_1}$ ,  $\frac{f_2}{F_2}$ , and  $\frac{f_{12}}{F_{12}}$ .

The boundaries of the ellipsoid in this figure are shown by the curves

AEDFBJICA. The plane  $\frac{f_2}{F_2} = 1$  is shown by DGBD, and the plane  $\frac{f_1}{F_1} = 1$  is shown

by AHDA. If the point representing the stresses is within the solid bounded by the ellipsoid and the planes, the orthotropic material will not fail. As the stresses are increased, the point representing them moves away from the origin. When this point reaches the boundary of the solid, the orthotropic material will fail.

It can readily be seen that the voids introduced in the isotropic material to make the orthotropic material need not be rectangular prisms, but might be ellipsoidal or any other shape without disturbing the validity of the theory. Also, the voids need not be equal in size nor uniformly spaced or oriented so long as, macroscopically, the material is orthotropic because of the manner in which the values of strengths,  $F$ , are determined. For the same reason, the solid material need not be isotropic but may be aeolotropic.

Comparison with the interaction equation. -- The author has suggested the use of an interaction equation to determine the strength of an orthotropic material subjected to a two-dimensional stress system (15). This equation is:

$$1 = \frac{f_1^2}{F_1^2} + \frac{f_2^2}{F_2^2} + \frac{f_{12}^2}{F_{12}^2} \quad (10)$$

This equation is identical to equation (9) except for the term

$$- \frac{f_1 f_2}{F_1 F_2}$$

It is represented in figure 5 by the sphere IKBMACI. This sphere lies outside the ellipsoid in the left-hand octant and within the ellipsoid in the right-hand octant. It intersects the ellipsoid on the lines ICA and CB. This equation has been checked by tensile, compressive, and shear tests in which the stress was applied at angles to one of the natural axes of the orthotropic material. These tests explored three lines on the ellipsoid. The tensile tests explored the line BLA in figure 5. It is evident from the figure that either of equations (9) or (10) should check the experiments very well, particularly if the shear strength of the material tested is low. The compressive tests explored a similar line in an octant not shown in figure 5. The shear tests explored the line JC in the figure. On this line, it is evident that equation (10) should yield greater values than equation (9). These tests are discussed subsequently. The results obtained fit the ellipsoid better than the sphere.

#### Strength at an Angle to a Natural Axis

Equation (9) is useful in the determination of the strength of an orthotropic material stressed at an angle to the direction of one of the natural axes. Consider two orthogonal axes, x and y, at an angle, α, to the natural axes, 1 and 2, as shown in figure 6. The stresses associated with these axes are  $f_x$ ,  $f_y$ , and  $f_{xy}$ . Then the stresses associated with the natural axes are given by the transformation equations (28):

$$\begin{aligned} f_1 &= f_x \cos^2 \theta + f_y \sin^2 \theta + 2f_{xy} \sin \theta \cos \theta \\ f_2 &= f_x \sin^2 \theta + f_y \cos^2 \theta - 2f_{xy} \sin \theta \cos \theta \\ f_{12} &= (f_y - f_x) \sin \theta \cos \theta + f_{xy}(\cos^2 \theta - \sin^2 \theta) \end{aligned} \quad (11)$$

Tensile strength.--If a tensile stress in the direction x exists alone, then  $f_y = f_{xy} = 0$  and equations (11) reduce to:

$$\begin{aligned} f_1 &= f_x \cos^2 \theta \\ f_2 &= f_x \sin^2 \theta \\ f_{12} &= -f_x \sin \theta \cos \theta \end{aligned} \quad (12)$$

Substituting these values in the first of equations (9) and replacing  $\underline{f_x}$  by  $\underline{F_x}$  to denote failure, the following equation results:

$$\frac{1}{F_x^2} = \frac{\cos^4 \theta}{F_1^2} + \left[ \frac{1}{F_{12}^2} - \frac{1}{F_1 F_2} \right] \sin^2 \theta \cos^2 \theta + \frac{\sin^4 \theta}{F_2^2} \quad (13)$$

This equation defines the curve BLA in figure 5. The exact position of this curve depends upon the ratio of  $F_1$  to  $F_2$ ; however, the curve passes through points A and B for all values of this ratio. The curve shown is the one for this ratio equal to unity.

Compressive strength.--Equations (13) can be used, also, for a compressive stress at an angle to one of the orthotropic axes if the associated values of  $\underline{F_1}$  and  $\underline{F_2}$  are employed.

Shear strength.--If a shear stress associated with axes  $\underline{x}$  and  $\underline{y}$  exists alone, then  $f_x = f_y = 0$  and equations (11) reduce to

$$\begin{aligned} f_1 &= f_{xy}^2 \sin \theta \cos \theta = f_{xy} \sin 2\theta \\ f_2 &= -f_{xy}^2 \sin \theta \cos \theta = -f_{xy} \sin 2\theta \\ f_{12} &= f_{xy} (\cos^2 \theta - \sin^2 \theta) = f_{xy} \cos 2\theta \end{aligned} \quad (14)$$

Substituting these values in the first of equations (9) and replacing  $\underline{f_{xy}}$  by  $\underline{F_{xy}}$  to denote failure, the following equation results:

$$\frac{1}{F_{xy}^2} = \left[ \frac{1}{F_1^2} + \frac{1}{F_1 F_2} + \frac{1}{F_2^2} \right] \sin^2 2\theta + \frac{\cos^2 2\theta}{F_{12}^2} \quad (15)$$

It should be remembered that one of the strengths  $\underline{F_1}$  or  $\underline{F_2}$  is a compressive strength and should be given the proper value. This equation defines the curve JC in figure 5. This curve moves according to the value of the ratio of  $\underline{F_1}$  to  $\underline{F_2}$ . It always passes through point C, but the position of point J depends upon this ratio. The curve shown is the one for this ratio equal to unity.

Compressive strength--specimen restrained.--In a structure or in a test in which the orthotropic material is subjected to a single stress  $f$ , the stresses  $\underline{f_y}$  and  $\underline{f_{xy}}$  may not be zero because of the restraint imposed by adjacent members

or by the testing machine. This may be true especially if  $\underline{f_x}$  is a compressive stress. The actual value of  $\underline{F_x}$ , of course, cannot usually be found because the values of  $\underline{f_y}$  and  $\underline{f_{xy}}$  are not known. However, the maximum possible value of  $\underline{F_x}$  can be found as follows.

Let

$$f_y = rf_x, \quad f_{xy} = sf_x$$

Then, equations (11) are written:

$$\begin{aligned} f_1 &= f_x \left[ \cos^2 \theta + r \sin^2 \theta + 2s \sin \theta \cos \theta \right] \\ f_2 &= f_x \left[ \sin^2 \theta + r \cos^2 \theta - 2s \sin \theta \cos \theta \right] \\ f_{12} &= f_x \left[ (r - 1) \sin \theta \cos \theta + s(\cos^2 \theta - \sin^2 \theta) \right] \end{aligned} \quad (16)$$

These values are substituted in the first of equations (9) and  $\underline{f_x}$  is maximized with respect to  $\underline{r}$  and  $\underline{s}$ . This process leads to:

$$F_x^2 = \frac{4}{3} \left[ F_1^2 \cos^4 \theta + F_2^2 \sin^4 \theta + (F_1 F_2 + 3F_{12}^2) \sin^2 \theta \cos^2 \theta \right] \quad (17)$$

This value of  $\underline{F_x}$  is limited by the second and third of equations (9). By using the second equation in the quadrant shown in figure 5,

$$f_2 = F_2$$

the second of equations (16) becomes

$$F_2 = f_x \left[ \sin^2 \theta + r \cos^2 \theta - 2s \sin \theta \cos \theta \right]$$

By using this equation with the others of equations (16) and again maximizing  $\underline{f_x}$  as before:

$$\underline{F_x} = 2 \frac{F_1^2 \cos^4 \theta + F_2^2 \sin^4 \theta + (F_1 F_2 + 3F_{12}^2) \sin^2 \theta \cos^2 \theta}{2F_2 \sin^2 \theta + F_1 \cos^2 \theta} \quad (18)$$

The third of equations (9) applied to the quadrant shown in figure 5 is:

$$f_1 = F_1$$

Thus the first of equations (16) becomes

$$F_1 = \underline{f_x} \left[ \cos^2 \theta + r \sin^2 \theta + 2s \sin \theta \cos \theta \right]$$

and the value of  $\underline{F_x}$  is:

$$\underline{F_x} = 2 \frac{F_1^2 \cos^4 \theta + F_2^2 \sin^4 \theta + (F_1 F_2 + 3F_{12}^2) \sin^2 \theta \cos^2 \theta}{2F_1 \cos^2 \theta + F_2 \sin^2 \theta} \quad (19)$$

The proper value of  $\underline{F_x}$  is the least value given by equations (17), (18), and (19). These equations can be used for either a tensile or compressive stress if the proper values of  $\underline{F_1}$  and  $\underline{F_2}$  are used.

The results of tests seldom reach the large values given by formulas (17), (18), and (19). A better approximation of the test conditions is obtained by assuming  $f_y = 0$  and  $\underline{f_{xy}}$  restrained; thus the value of  $\underline{r}$  in equations (16) is assumed to be zero. This assumption results in:

$$\underline{F_x}^2 = \frac{F_1^2 F_2^2 \cos^4 \theta + 2 \left[ 2(F_1^2 + F_1 F_2 + F_2^2) F_{12}^2 - F_1^2 F_2^2 \right] \sin^2 \theta \cos^2 \theta + F_1^2 F_2^2 \sin^4 \theta}{F_2^2 \cos^4 \theta + (3F_{12}^2 + F_1 F_2) \sin^2 \theta \cos^2 \theta + F_1^2 \sin^4 \theta} \quad (20)$$

Shear strength--specimen restrained.--An equation for the shear strength when the panel is completely restrained can be obtained in a similar way. Equations (16) become:

$$\begin{aligned} f_1 &= f_{xy} \left[ a \cos^2 \theta + b \sin^2 \theta + 2 \sin \theta \cos \theta \right] \\ f_2 &= f_{xy} \left[ a \sin^2 \theta + b \cos^2 \theta - 2 \sin \theta \cos \theta \right] \\ f_{12} &= f_{xy} \left[ (b - a) \sin \theta \cos \theta + \cos^2 \theta - \sin^2 \theta \right] \end{aligned} \quad (21)$$

in which

$$a = \frac{f_x}{f_{xy}}$$

and

$$b = \frac{f_y}{f_{xy}}$$

and the equation resulting from the maximization of  $f_{xy}$  with respect to  $a$  and  $b$  is:

$$F_{xy}^2 = F_{12}^2 \cos^2 2\theta + \frac{1}{3} (F_1^2 - F_1 F_2 + F_2^2) \sin^2 2\theta \quad (22)$$

It should be remembered that one of the strengths,  $F_1$  or  $F_2$ , is a compressive strength and should be given the proper value.

### Macroscopic Isotropic Materials

The orthotropic materials discussed have been made by introducing voids into and isotropic material. If these voids are heterogeneously dispersed in an isotropic material, the resulting material will be, macroscopically, isotropic. The tensile strength of such a material will have the same value no matter in what direction the stress is applied. It follows that  $F_1 = F_2 = F$  and that the value of  $F_x$  given by equation (13) is independent of  $\alpha$ . This condition is

obtained if the right-hand member of this equation is a perfect square. To obtain this condition

$$\frac{1}{F_{12}^2} = \frac{3}{F^2}$$

or

$$F_{12} = \frac{F}{\sqrt{3}} = 0.577 F$$

This relation can also be obtained directly from the Henky-von Mises theory. It is reasonably accurate for most ductile materials.

For this material, the natural axes, of course, have no meaning and the axes of reference can be chosen in any direction. If the axes are chosen in the directions of the principal axes of stress, the axis for shear stress is eliminated. The ellipsoid in figure 5 becomes the ellipse IJBFD EA, which is the ellipse determined by the Henky-von Mises theory; however, there is the great difference that this ellipse is now cut by the lines BD and AD. It is noteworthy that the ellipse, cut in this manner, agrees very well with the results of tests on metals (1,3,8,23,24).

#### Comparison With Experimental Data

A considerable number of data concerned with the strength of orthotropic materials stressed at angles to the natural axes has been obtained. A limited number of these data will be used for comparison with the theory developed. Those used are taken from Forest Products Laboratory Reports Nos. 1328 (15) on plywood and 1803 (30) on fiberglass laminate and from Rowse's thesis (20) on Douglas-fir wood. The first two reports contain determinations of the tensile, compressive, and shear strengths associated with the natural axes of the materials, and these values were used where indicated in the formulas. Rowse determined proportional limits rather than strengths, and the theory, therefore, does not rigidly apply. He did not report the shear stress at proportional limit, and it was estimated for the purpose of this comparison.

#### Plywood

Tensile tests.--The tensile specimens were 16 inches long, and of the thickness of the laminate. The maximum sections at the ends were 1-1/2 inches wide and 2-7/8 inches long. The minimum section at the center was 0.8 inch wide and 2-1/2 inches long. The maximum and minimum sections were connected by circular



arcs of 20-inch radius tangent to the minimum section. The method of test is described in the reference. The data chosen for comparison are those for three ply plywood made of 1/16-inch veneers. The strength values for substitution in the formulas are:

$$F_1 = 11,034 \text{ (table 10, Report No. 1328-B (17))}$$

$$F_2 = 6,300 \text{ (table 10, Report No. 1328-B)}$$

$$F_{12} = 1,410 \text{ (table 18, Report No. 1328-C (18))}$$

These values substituted in equation (13) yield the curve shown in figure 7. The points shown in the figure represent the average values given in table 10 of Report 1328-B (17). Equation (13) was used because a tensile specimen, being long, is not restrained by the grips of the testing machine. Remarkable agreement was obtained between the test values and the theory. Perfect agreement could not be expected because of stress concentrations introduced by the shape of the specimen (22).

Compression.--The data chosen for comparison with the theory are those obtained from tests on three-ply plywood. Compressive specimens have to be comparatively short so that they will be elastically stable. They are, therefore, likely to be restrained by the testing machine in two ways. The action of Poisson's ratios is restrained by friction with the heads of the machine, and shear strains are restrained because the heads are guided. This second kind of restraint could have been removed by employing rollers, as illustrated in figure 8, instead of placing the specimen between the heads, as shown in figure 9. The strength values substituted in the equations are:

$$F_1 = 5,125 \text{ (table 2, Report No. 1328-A)}$$

$$F_2 = 2,480 \text{ (table 2, Report No. 1328-A)}$$

$$F_{12} = 1,410 \text{ (table 18, Report No. 1328-C)}$$

These values were substituted in equations (13), (17), (18), (19), and (20), and the curves plotted in figure 10 were obtained. Equation (13) yields values of compressive strength that the theory predicts if the specimen is not restrained in any way. Equations (17), (18), and (19) yield values consistent with complete restraint, and equation (20) yields values consistent with shear restraint alone. The plotted experimental values were taken from table 2 of Report No. 1328-A (16) and follow the curve of equation (20) with reasonable accuracy.

Shear.--The apparatus used in making the shear tests on three-plyplywood was considered unsatisfactory. The results of these tests, however, agree quite well with the theory. The values substituted in the formulas for positive angles are:

$$F_1 = 11,034 \text{ (tension) (table 10, Report No. 1328-B)}$$

$$F_2 = 2,480 \text{ (compression) (table 2, Report No. 1328-A)}$$

$$F_{12} = 1,410 \text{ (table 18, Report No. 1328-C)}$$

and for negative angles:

$$F_1 = 5,125 \text{ (compression) (table 2, Report No. 1328-A)}$$

$$F_2 = 6,300 \text{ (tension) (table 10, Report No. 1328-B)}$$

$$F_{12} = 1,410 \text{ (table 18, Report No. 1328-C)}$$

These values were substituted in equations (15) and (22), and the curves plotted in figure 11 were obtained. The plotted points represent the average values for a three-plyplywood given in table 18, Report No. 1328-C (18).

Some shear tests were made on five-plyyellow-poplarplywood (1/16-inch veneers) with a better apparatus. The values substituted in the formulas for comparison with the tests are for positive angles:

$$F_1 = 10,241 \text{ (tension) (table 11, Report No. 1328-B)}$$

$$F_2 = 2,760 \text{ (compression) (table 3, Report No. 1328-A)}$$

$$F_{12} = 1,460 \text{ (table 20, group 3, Report No. 1328-C)}$$

and for negative angles:

$$F_1 = 4,230 \text{ (compression) (table 3, Report No. 1328-A)}$$

$$F_2 = 7,255 \text{ (tension) (table 11, Report No. 1328-B)}$$

$$F_{12} = 1,460 \text{ (table 20, group 3, Report No. 1328-C)}$$

These values were substituted in equations (15) and (22), and the curves were plotted as shown in figure 12. The experimental values plotted in this figure are obtained from table 20 (group 3) of Report No. 1328C (18).

In both of these figures (11 and 12) the experimentally determined points lie between the curves representing restraint-free and fully restrained tests. Pure shear is difficult to obtain in a test. , Part of this difficulty is explained by the great distances between some of the curves for unrestrained and completely restrained test conditions.

#### Glass Fabric Laminate

Glass fabric laminate 143-114 was chosen for comparison with the theory because of its marked difference in directional properties. Most of the glass fibers in the cloth from which this laminate was made ran in one direction, and the cloth layers were oriented so that this direction was common to all the layers. The values used in the formulas and for comparison with the theory are taken from Forest Products Laboratory Report No, 1803-A (31), table 5.

Tension, -- The values for substitution in the equations are:

$$F_1 = 87,320$$

$$F_2 = 9,880$$

$$F_{12} = 11,230$$

These values were substituted in equation (13), and the curve was plotted in figure 13, The experimental values plotted in this figure were obtained from table 5, column 7, of Report 1803-A. Remarkable agreement is obtained with the theory.

Compression. -- The values for substitution in the equations are:

$$F_1 = 56,800$$

$$F_2 = 20,950$$

$$F_{12} = 11,230$$

These values were substituted in equation (13), and the curve was plotted as shown in figure 14. The experimental values plotted in this figure are taken from table 5, column 13, of Report 1803-A. The specimens were 1 inch wide and 4 inches long and were supported against elastic instability as shown in figure 3 of Forest Products Laboratory Report No. 1803. Good agreement is obtained between the experimental values and equation (13), as is shown in figure 14. It can be assumed, therefore, that this type of specimen is not greatly restrained by the testing machine.

Shear.--The values for substitution in the equation for positive angles are:

$$F_1 = 87,320 \text{ (tension)}$$

$$F_2 = 20,950 \text{ (compression)}$$

$$F_{12} = 11,230$$

and for negative angles they are:

$$F_1 = 56,800 \text{ (compression)}$$

$$F_2 = 9,880 \text{ (tension)}$$

$$F_{12} = 11,230$$

These values were substituted in equation (15), and the resulting curve was plotted as shown in figure 15. The experimental values plotted in this figure are taken from table 5, column 18, of Report No. 1803-A. All of the experimental values, except one, lie below the curve. The lowest one is about 28 percent below the theoretical value. It is possible that stress concentrations due to the method of test are responsible for these low values. The test apparatus is illustrated in figures 6, 7, and 8 of Report No. 1803. The shear loads are applied to the faces of the laminate instead of to the edges. This results in a complicated stress distribution at the edges of the part of the specimen that is tested. This complicated stress situation may lead to concentrations that decrease the load at failure.

#### Douglas-fir in Compression

The data used for comparative purposes is that of Rowse's thesis (20). The proportional limit of the Douglas-fir used by Rowse is not given in his thesis and therefore is estimated. Forest Products Laboratory Report No. 1801 (14) presents shear stress-strain curves for a few species of wood, including

Douglas-fir. Examination of these curves indicates that the proportional limit stress in shear of Douglas-fir is closely equal to one-half of the shear strength. The shear strength of the Douglas-fir used by Rowse is estimated by means of U.S. Department of Agriculture Technical Bulletin No. 479 (9) by using values for Rocky Mountain-type Douglas-fir that are closest to those obtained by Rowse. The following tabulation shows the known values and those estimated:

<u>Property</u> (P.s.i.)	<u>Values by</u> <u>Bulletin</u> <u>No. 479</u>	<u>Values</u> <u>estimated</u> <u>by Rowse</u>
Compression proportional limit stress, parallel	4,660	4,120
Compression proportional limit stress, perpendicular	820	773
Shear strength, parallel	1,070	1,008
Shear proportional limit stress, parallel (estimated to be 1/2 of shear strength)	535	504

The value of shear strength given for the Douglas-fir used by Rowse is estimated by use of the ratios of the proportional limit stresses in compression given by Technical Bulletin No. 479 to those given by Rowse. Thus the values to be substituted in the equations are:

$$F_1 = 4,120$$

$$F_2 = 773$$

$$F_{12} = 504$$

These values were substituted in equations (13), (17), (18), (19), and (20), and the resulting curves were plotted as shown in figure 16. The experimental values plotted in this figure were taken from Rowse's thesis.

The specimens tested by Rowse were notched, as a beam in a truss would be notched to receive the end of a diagonal member, and, therefore, were considerably restrained by the method of test. The test values lie between the curves for shear restraint alone (equation 20) and full restraint (equations 17, 18, and 19), as might be expected.

The dashed curve in figure 16 is a plot of the Hankinson equation. It fits the experimental data a little better than equation (20) due to the restraint

imposed on the specimens, It might be pointed out that equation (13) reduces to the Hankinson equation if

$$F_{12}^2 = \frac{F_1 F_2}{3}$$

For these particular data, this relationship yields a value of  $F_{12} = 1,030$ .

This value is, of course, too great because it includes the restraint placed on the specimen due to the method of test.

### Conclusions

The experimental values confirm the theory as closely as can be expected. All of the tensile tests and the compressive tests on glass fabric laminate confirm it with remarkable accuracy. The compressive tests on plywood confirm the theory if it is assumed that the testing machine applied shear stresses to the specimen, due to friction between the specimen and the heads of the machine. The remaining tests agree with the theory as closely as can be expected. The lack of agreement is probably due to inadequate methods of test. Further confirmation should be obtained by tests imposing combined tensile stress in two directions and shear.

### Literature Cited

- (1) American Society of Metals.  
1948. Fracturing of Metals. Seminar on the Fracturing of Metals Held During the 29th Natl. Metal Cong. and Expo. in Chicago, Oct. 1948, 311 pp. Am. Soc. Metals, Cleveland.
- (2) Ayers, Q. C.  
1920. Engin. News-Record. Univ. of Miss. (Sept. 30.)
- (3) Chance Vought Aircraft.  
Verification of Design Allowable Stresses for Panels Under Biaxial Compression. Chance Vought Aircraft Rpt. MP-2016. Stratford, Conn.
- (4) Dewell, H. D.  
1920. Engin. News-Record. (Oct. 24.)
- (5) Hare, M. A.  
1912. Engin. News. (Aug. 1.)
- (6) Jacoby, H. S.  
1909. Structural Details or Elements of Design in Heavy Framing. Wiley.

- (7) Jenkins, C. F.  
1920. Report. on Materials of Construction Used in Aircraft and Aircraft Engines, 162 pp., illus. H. M. Stationary Off., London, England.
- (8) Marin, Joseph.  
1942. Mechanical Properties of Materials and Design. 273 pp., illus. McGraw-Hill.
- (9) Markwardt, L. J., and Wilson, T. R. C.  
1935. Strength and Related Properties of Woods Grown in the United States, U.S. Dept. Agr. Tech. Bul. 479, 99 pp., illus.
- (10) Martel, R. R.  
1920. Engin. News-Record. Calif. Inst. Tech. (Nov. 11.)
- (11) Nadai, Arpad.  
1933. Theories of Strength. Trans. Amer. Soc. Mech. Engin. Appl. Mechanics 1 (3): 111-129.
- (12) \_\_\_\_\_  
1931. Plasticity. A Mechanics of the Plastic State of Matter. Chapter 13 of Engin. Societies Monog., 349 pp., illus. McGraw-Hill.
- (13) Norris, C. B.  
1939. Elastic Theory of Wood Failure. Trans. Amer. Soc. Mech. Engin. 61 (3): 259-261.
- (14) \_\_\_\_\_, Werren, Fred, and McKinnon, P. F.  
1961. The Effect of Veneer Thickness and Grain Direction on the Shear Strength of Plywood. Forest Prod. Lab. Rpt. 1801, 30 pp., illus.
- (15) \_\_\_\_\_, and McKinnon, P. F.  
1956. Compression, Tension. and Shear Tests on Yellow-poplar Plywood Panels of Sizes That Do Not Buckle With Tests Made at Various Angles to the Face Grain. Forest Prod. Lab. Rpt. 1328, 26 pp., illus.
- (16) \_\_\_\_\_, and McKinnon, P. F.  
1956. Supplement to Compression, Tension, and Shear Tests on Yellow-poplar Plywood Panels of Sizes That Do Not Buckle With Tests Made at Various Angles to the Face Grain (CompressionTests). Forest Prod. Lab. Rpt. 1328-A, 5 pp., illus.
- (17) \_\_\_\_\_, and McKinnon, P. F.  
1956. Supplement to Compression, Tension, and Shear Tests on Yellow-poplar Plywood Panels of Sizes That Do Not Buckle With Tests Made at Various Angles to the Face Grain (TensionTests). Forest Prod. Lab. Rpt. 1328-B, 8 pp., illus.

- (18) Norris, C. B., and McKinnon, P. F.  
1956. Supplement to Compression, Tension, and Shear Tests on Yellow-poplar Plywood Panels of Sizes That Do Not Buckle With Tests Made at Various Angles to the Face Grain (Shear Tests). Forest Prod. Lab. Rpt. 1328-C, 11 pp., illus.
- (19) Osgood, W. R.  
1928. Compressive Stress on Wood Surfaces Inclined to the Grain. Engin. News-Record. (Feb. 9.)
- (20) Rowse, R. C.  
1923. The Strength of Douglas-fir in Compression at Various Angles to the Grain. Thesis for Degree of Bachelor in Civil Engin. at Wash. Univ., St. Louis, Mo.
- (21) Simpson, T. R.  
1920. Engin. News-Record. Univ. of Calif. (Sept. 30.)
- (22) Smith, C. Bassel.  
1949. Effect of Hyperbolic Notches on the Stress Distribution in a Wood Plate. Quart. of Appl. Math, 6 (4): 452-56.
- (23) Thomsen, E. G., Lotze, I., and Dorn, J. E.  
1948. Fracture Strength of 755-T Aluminum Alloy Under Combined Stress. Natl. Advisory Com. for Aeronaut. Tech. Note 1551, 30 pp.
- (24) \_\_\_\_\_, Cunningham, D. M., and Dorn, J. E.  
1947. Fracture of Some Aluminum Alloys Under Combined Stress. Trans. Amer. Soc. Mech. Engin. 69 (2): 81-87.
- (25) Timoshenko, Stephen.  
1936. Theory of Elastic Stability. Section on Ultimate Strength of Buckled Plates. pp. 395-400. McGraw-Hill.
- (26) U.S. Air Service.  
1921. Investigation of Crushing Strength of Spruce at Various Angles of Grain. Air Serv. Inform. Cir. III (259), 15 pp., illus.
- (27) U.S. Forest Products Laboratory.  
1960. Effect of Ten Repetitions of Stress on the Bending and Compressive Strengths of Sitka Spruce and Douglas-fir. Forest Prod. Lab. Rpt. 1320, 7 pp., illus.
- (28) \_\_\_\_\_  
1957. Stress-Strain Relations in Wood and Plywood Considered as Orthotropic Materials. Forest Prod. Lab. Rpt. 1503, 33 pp., illus.
- (29) Werren, Fred.  
1957. Effect of Prestressing in Tension or Compression on the Mechanical Properties of Two Glass-Fabric-Base Plastic Laminates. Forest Prod. Lab. Rpt. 1811.



(30) Werren, Fred, and Norris, C. B.

1956. Directional Properties of Glass-Fabric-BasePlastic Laminate  
Panels of Sizes That Do Not Buckle. Forest Prod. Lab. Rpt.  
1803, 24 pp., illus.

(31) \_\_\_\_\_

1956. Supplement to Directional Properties of Glass-Fabric-BasePlastic  
Laminate Panels of Sizes That Do Not Buckle. Forest Prod.  
Lab. Rpt. 1803-A, 7 pp., illus.

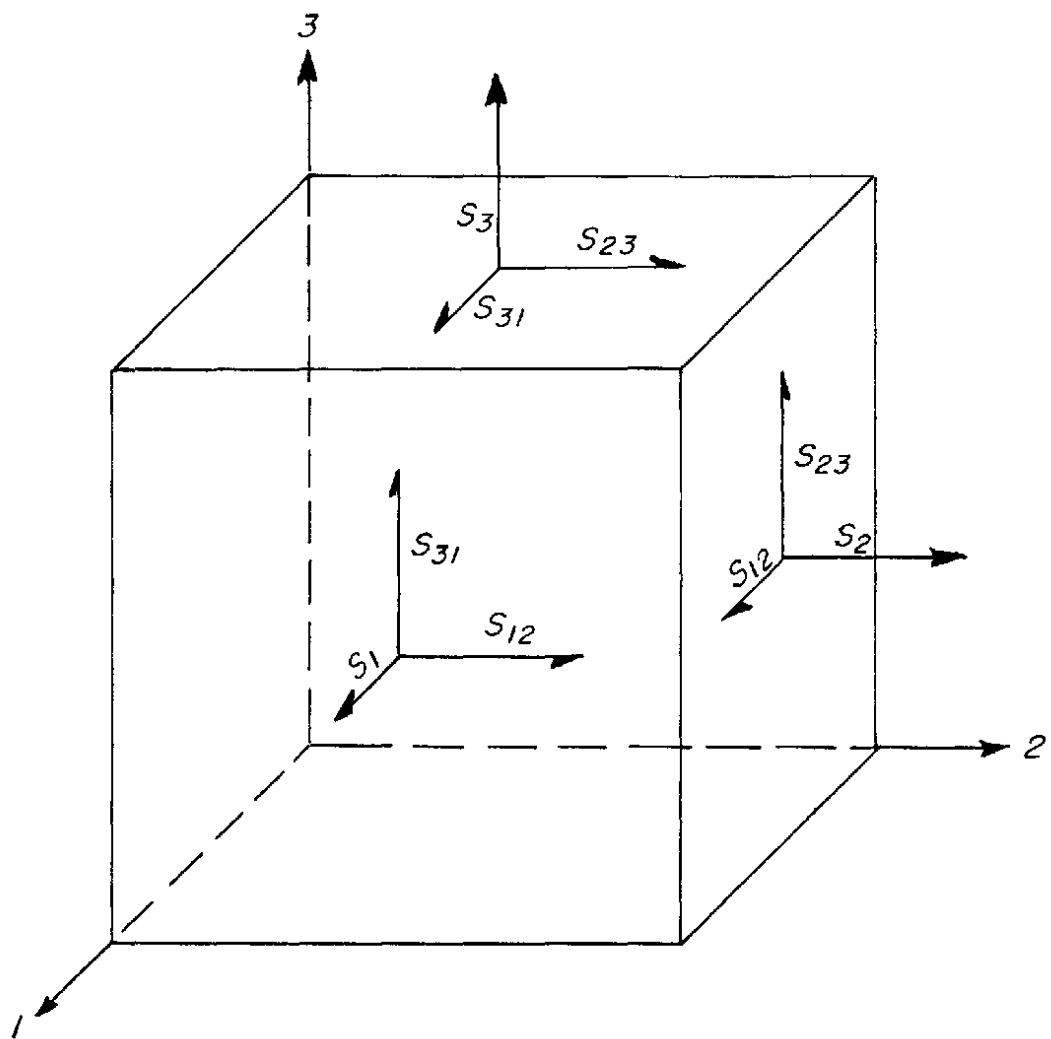


Figure 1.--Illustration of stresses within a material.

Z M 85010 F

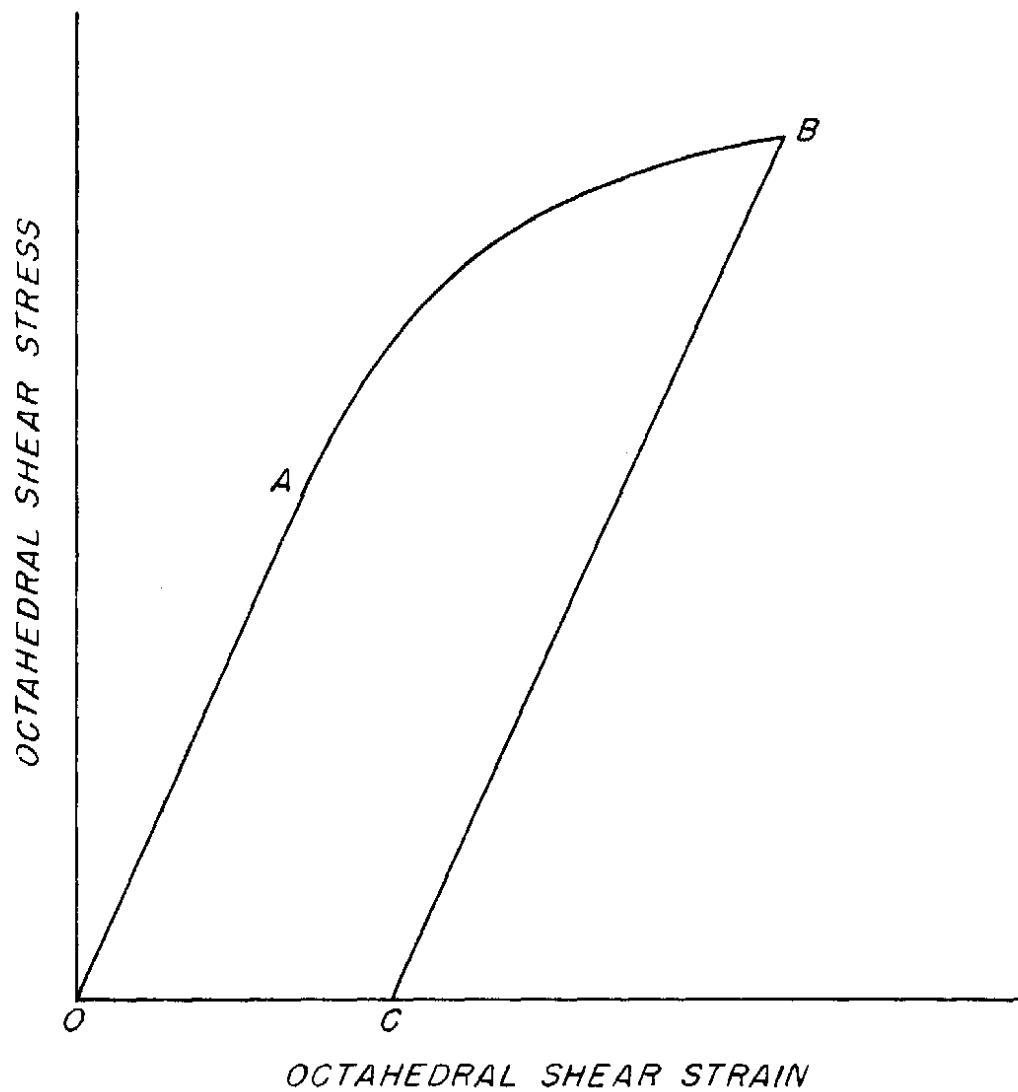


Figure 2.--Illustrative stress-strain curve.

Z M 85011 F

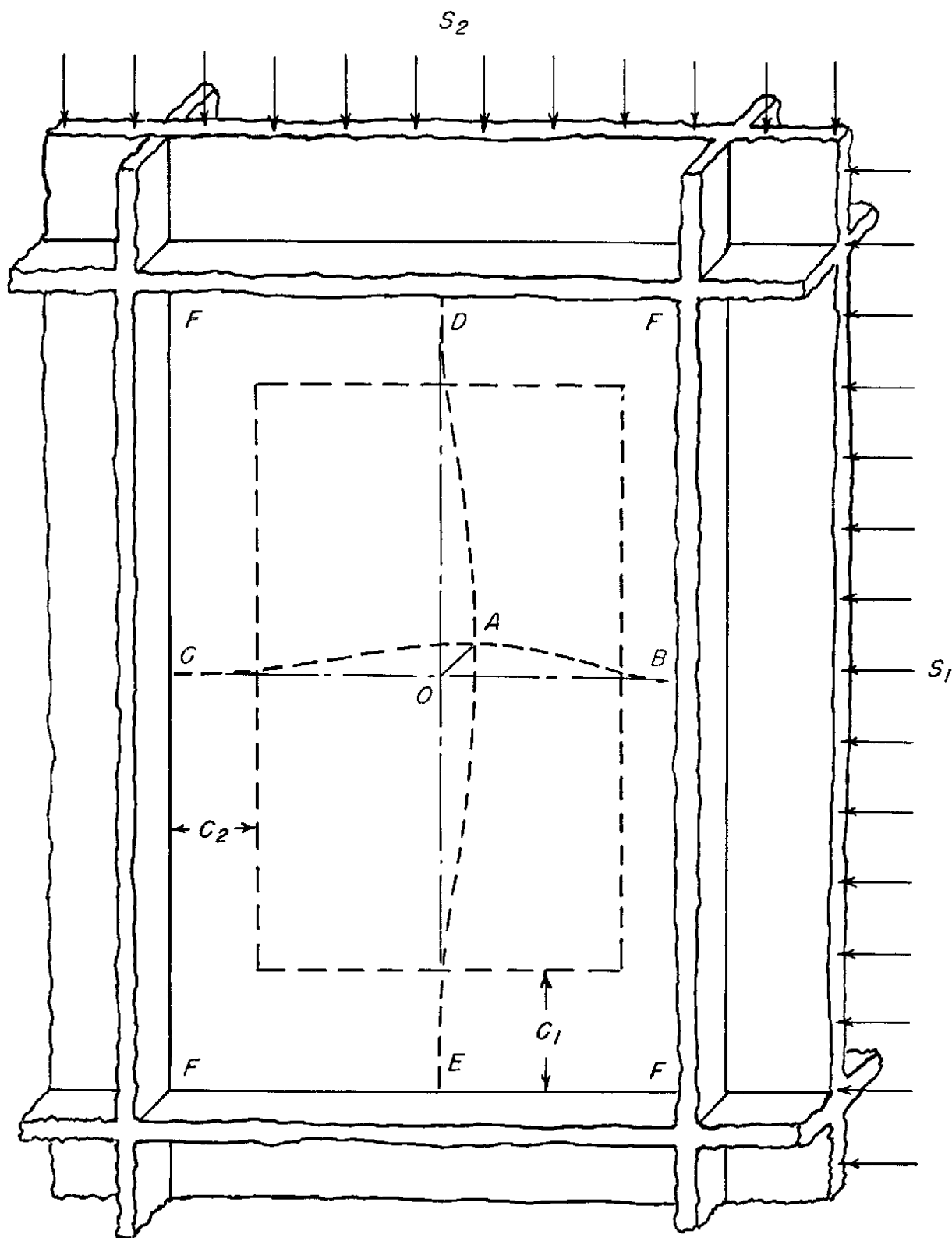


Figure 3.—Single wall broken from the orthotropic material.

Z M 85012 F

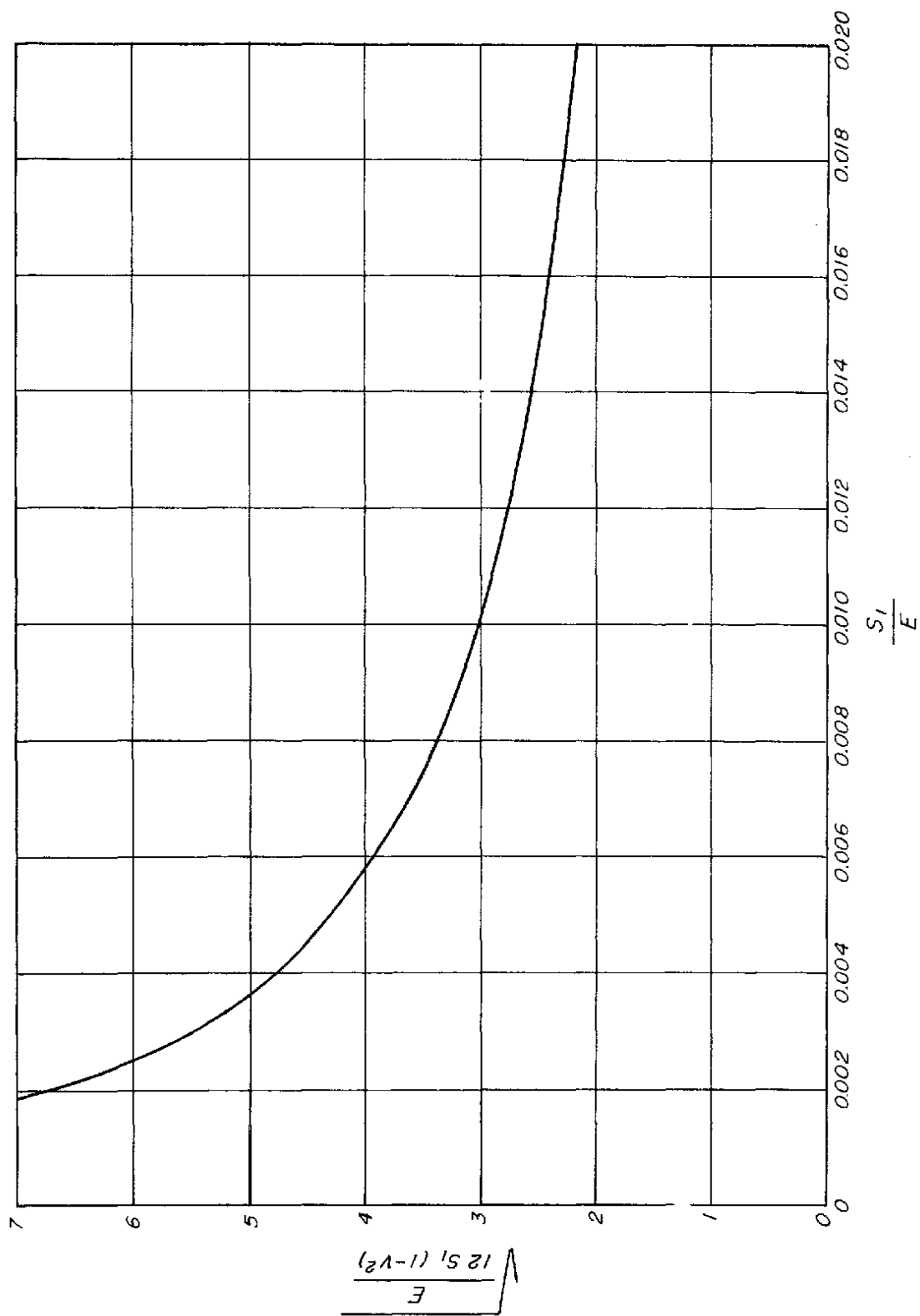


Figure 4.--Plot indicating change of width of strip with stress  $\nu = 0.3$ .

Z M 85013 F



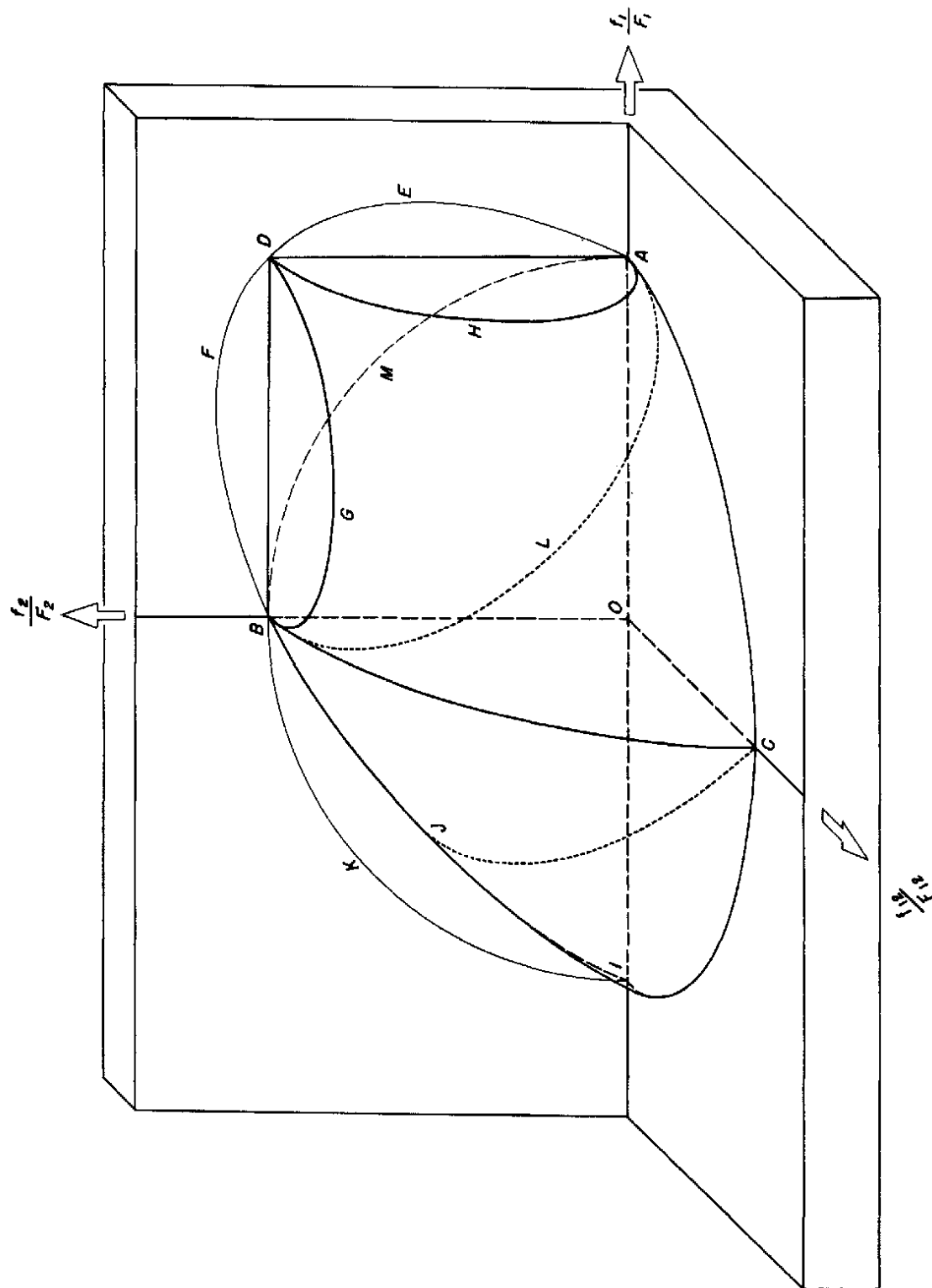


Figure 5.--Surface of limiting stress.

Z M 85014 F

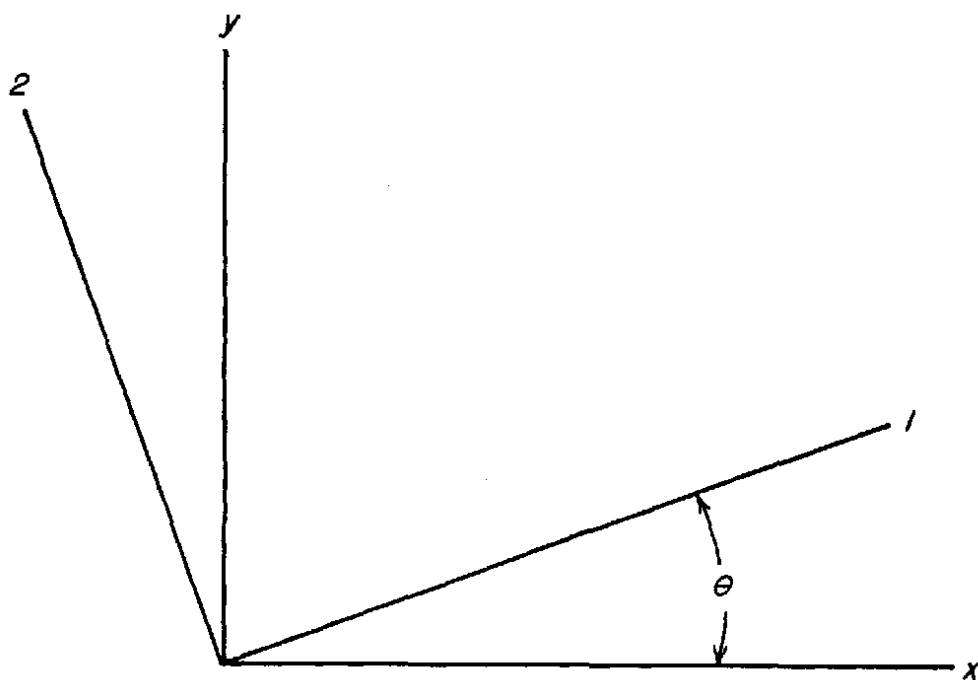


Figure 6.--Illustration of choice of axes.

Z M 85015 F



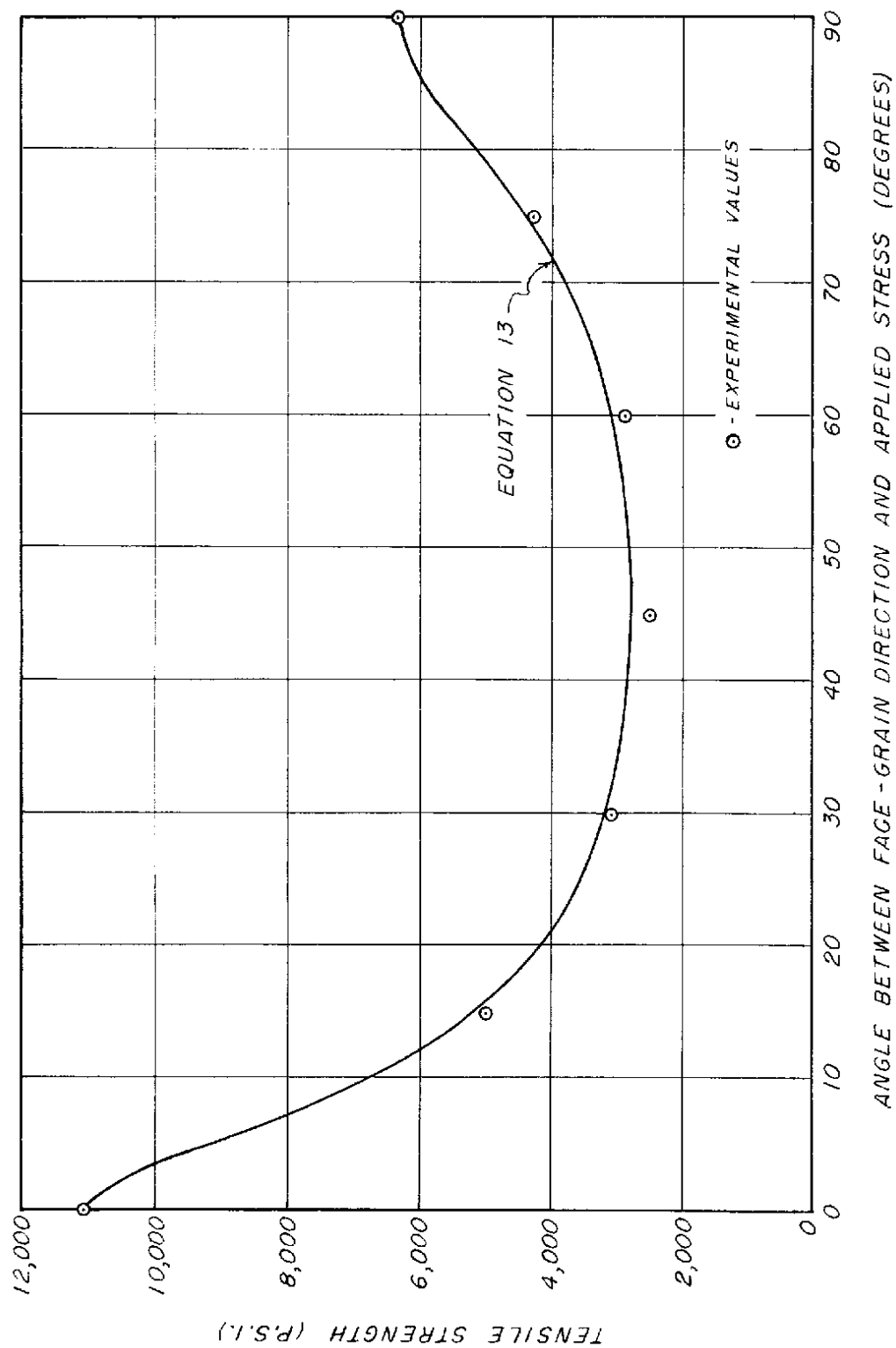


Figure 7.--Tensile strength of three-ply yellow-poplar plywood at various angles to the face grain.

Z M 85016 F

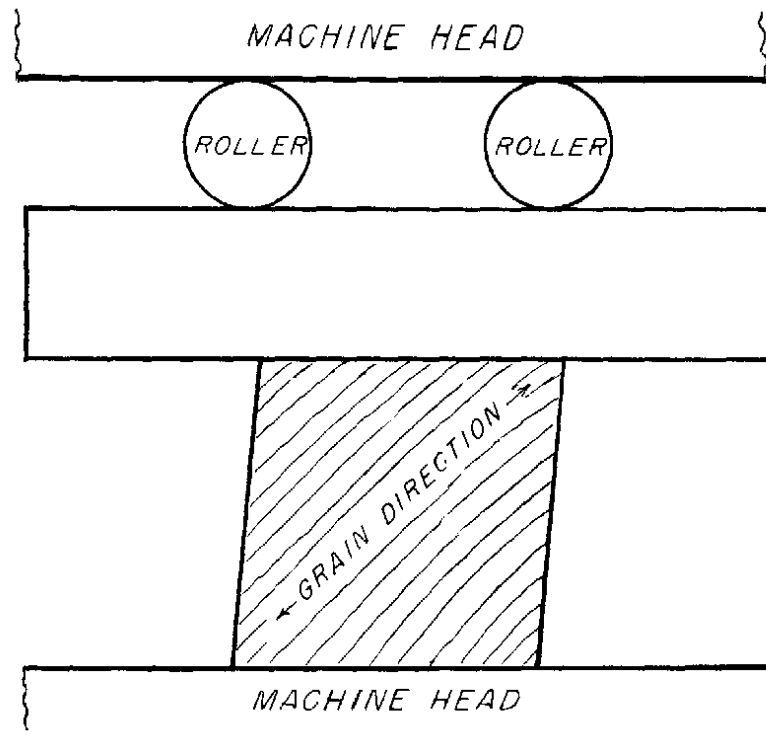


Figure 8 (top).--Illustration of a method of removing shear restraint in a compressive test.

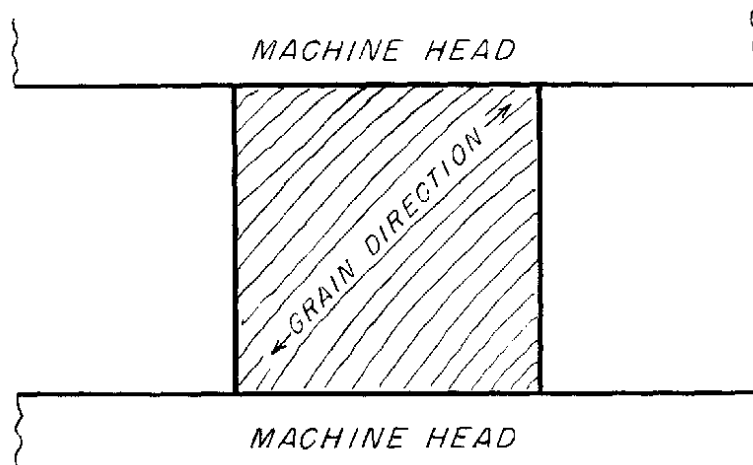


Figure 9 (bottom) .--Illustration of shear restraint in a compressive test.

Z M 85017 F

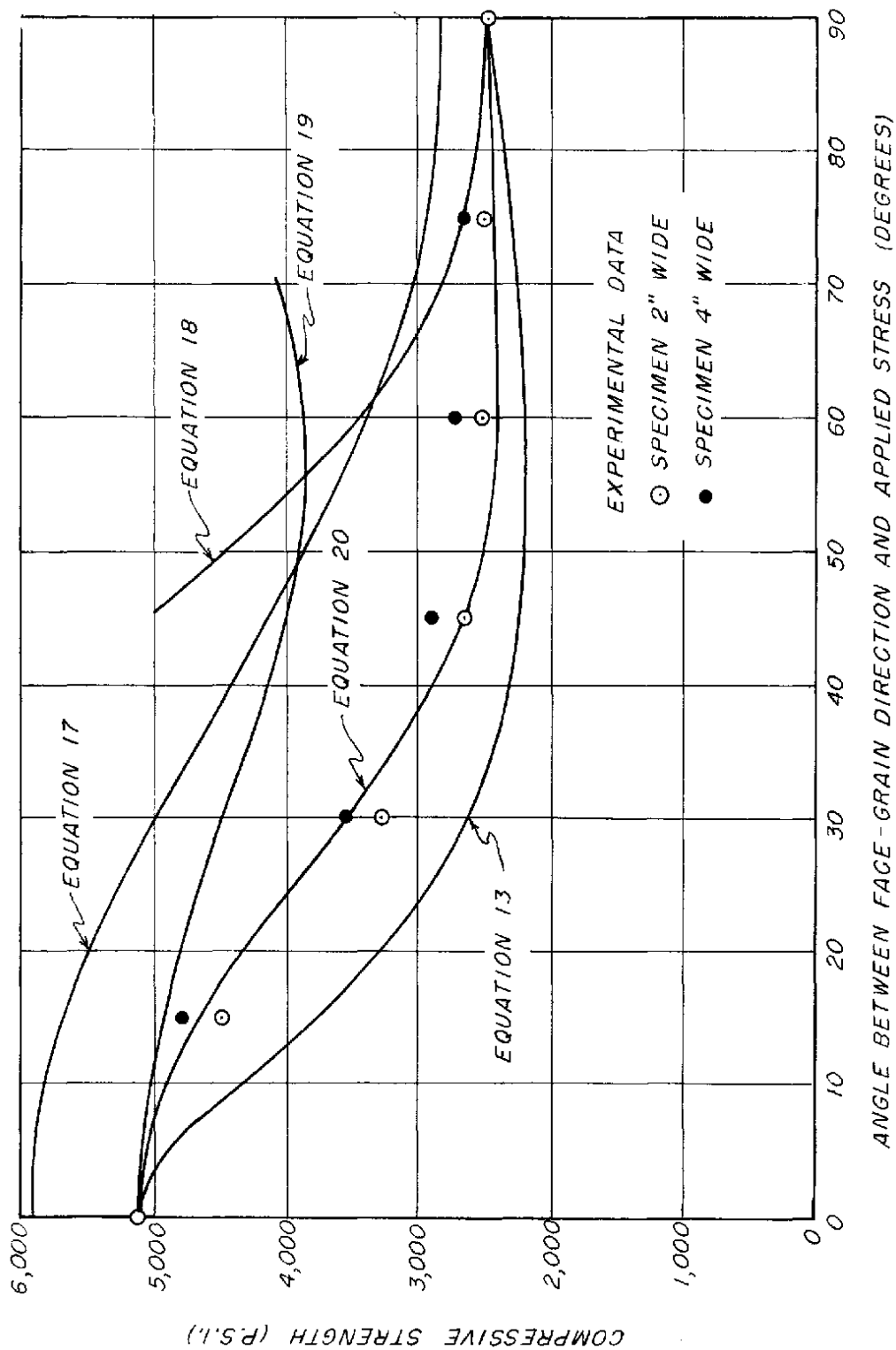


Figure 10.--Compressive strength of three-ply yellow-poplar plywood at various angles to the face grain.

Z M 85018

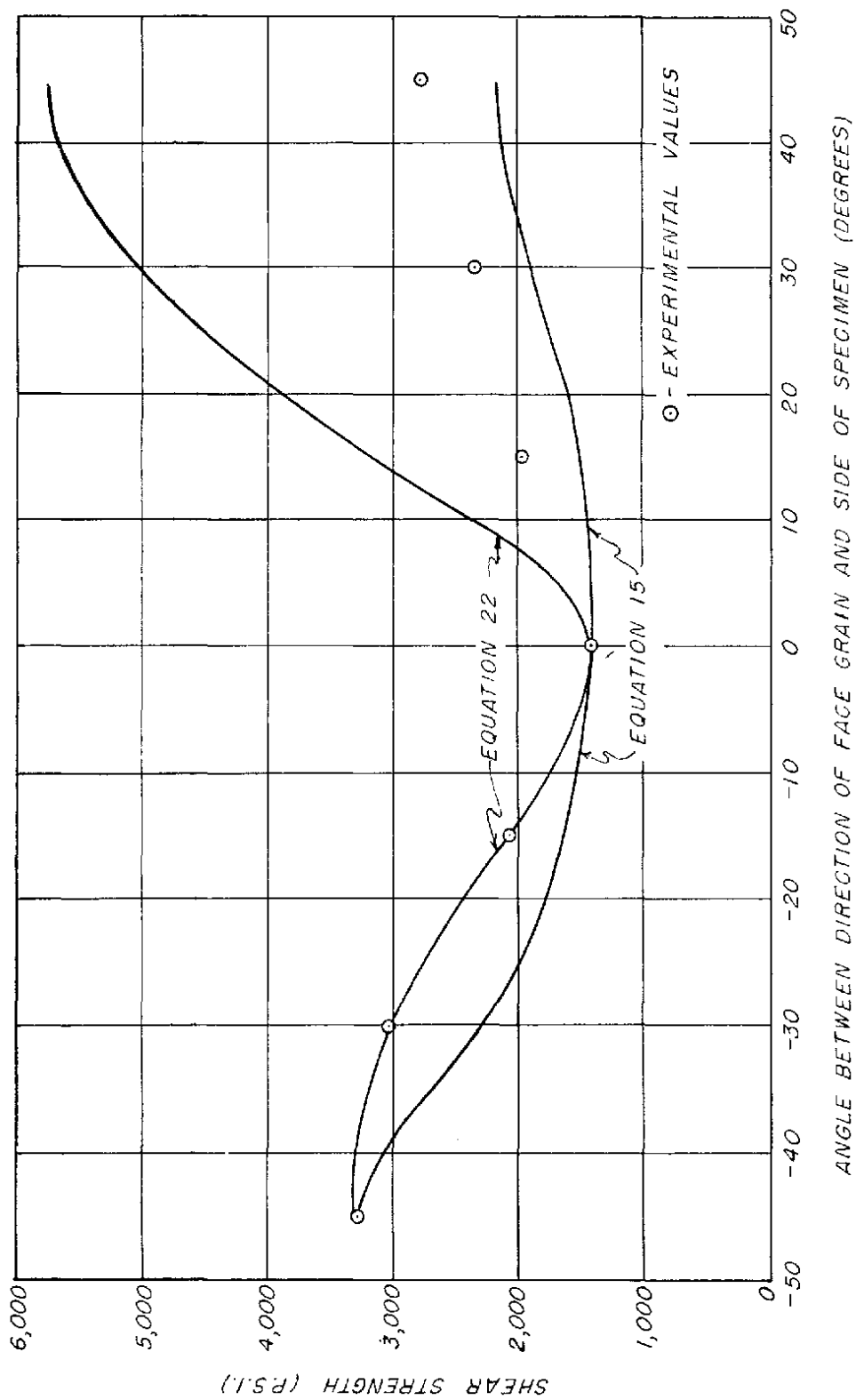


Figure 11.--Shear strength of three-ply yellow-poplar plywood at various angles with the face grain.

Z M 85019 F

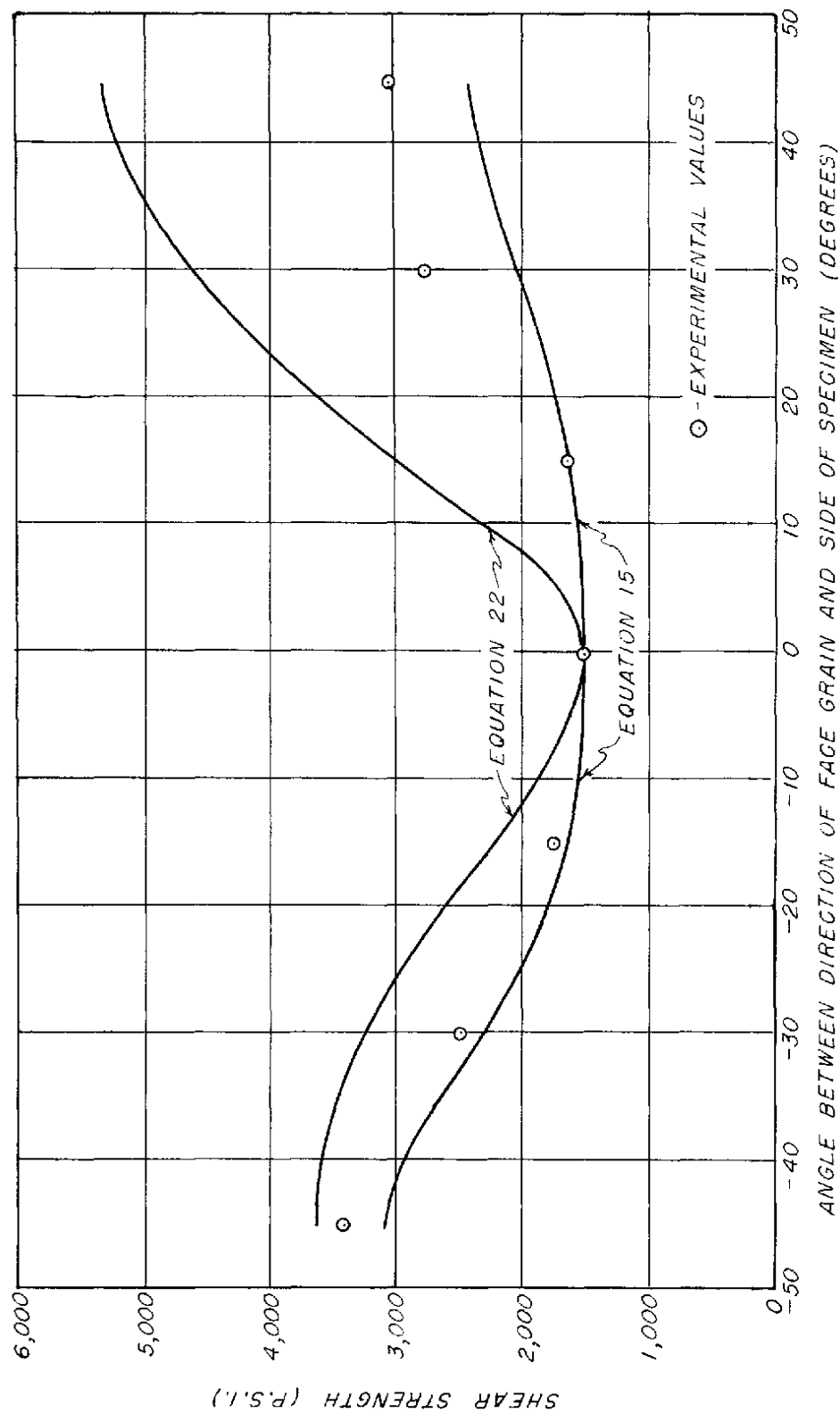


Figure 12.--Shear strength of five-ply (1/16-inch veneers) yellow-poplar plywood at various angles with the face grain.

Z M 85020 F

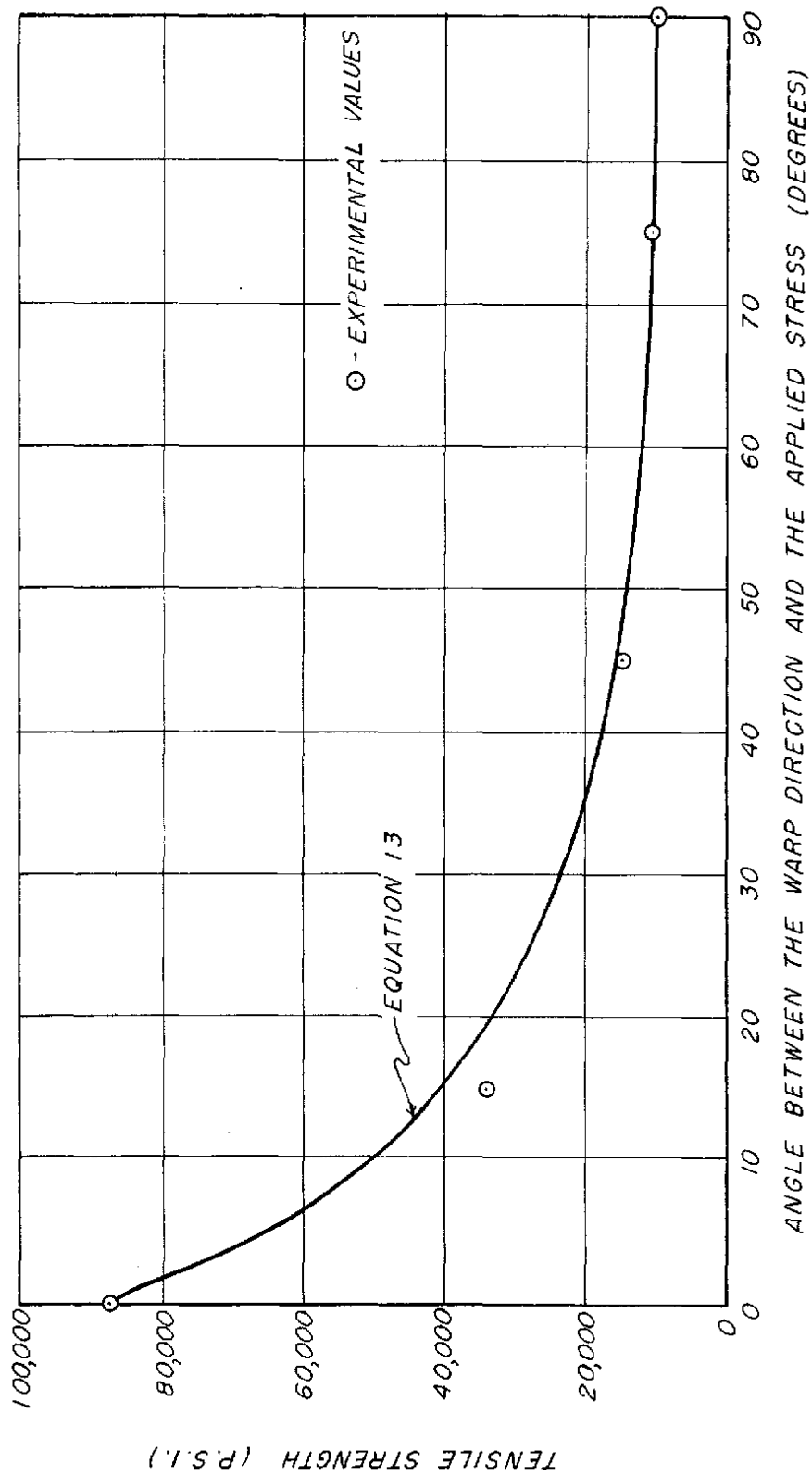


Figure 13.--Tensile strength of 143-144 glass fabric laminate at various angles to the warp.

Z M 85021 F

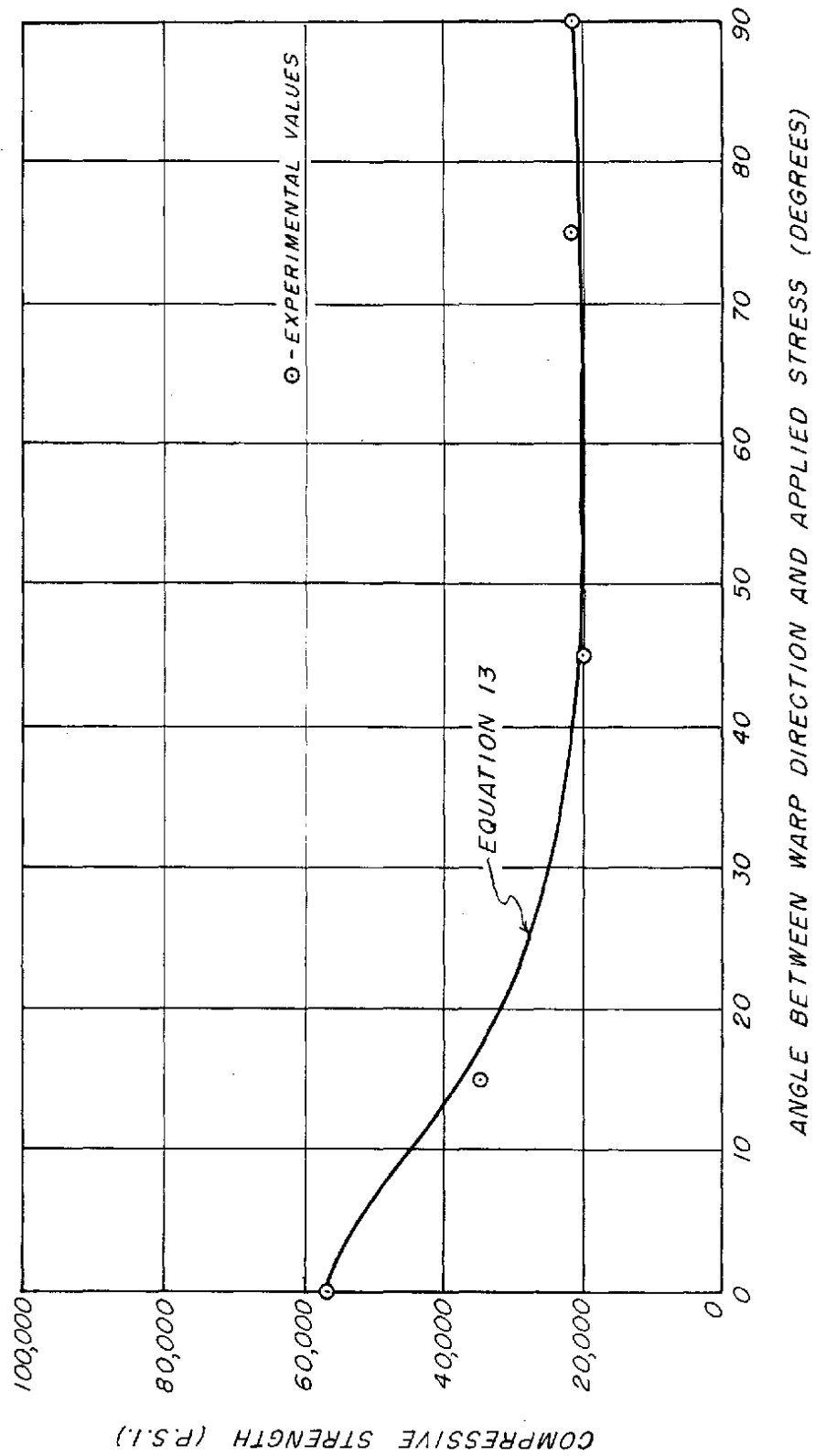


Figure 14.--Compressive strength of 143-144 glass fabric laminate at various angles to the warp.

Z M 85022 F

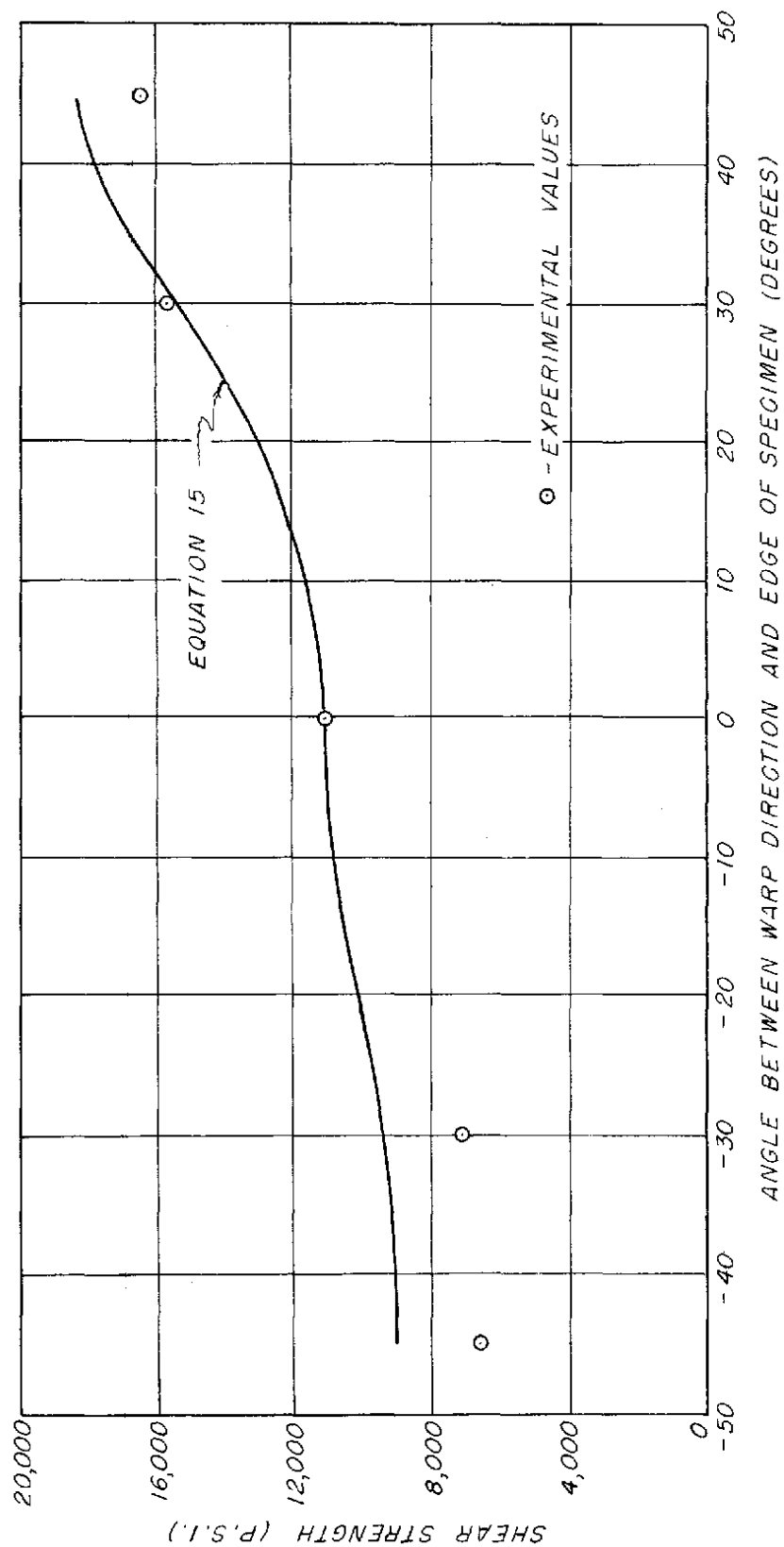


Figure 15.--Shear strength of 143-144 glass fabric laminate at various angles to the warp.

Z M 85023 F



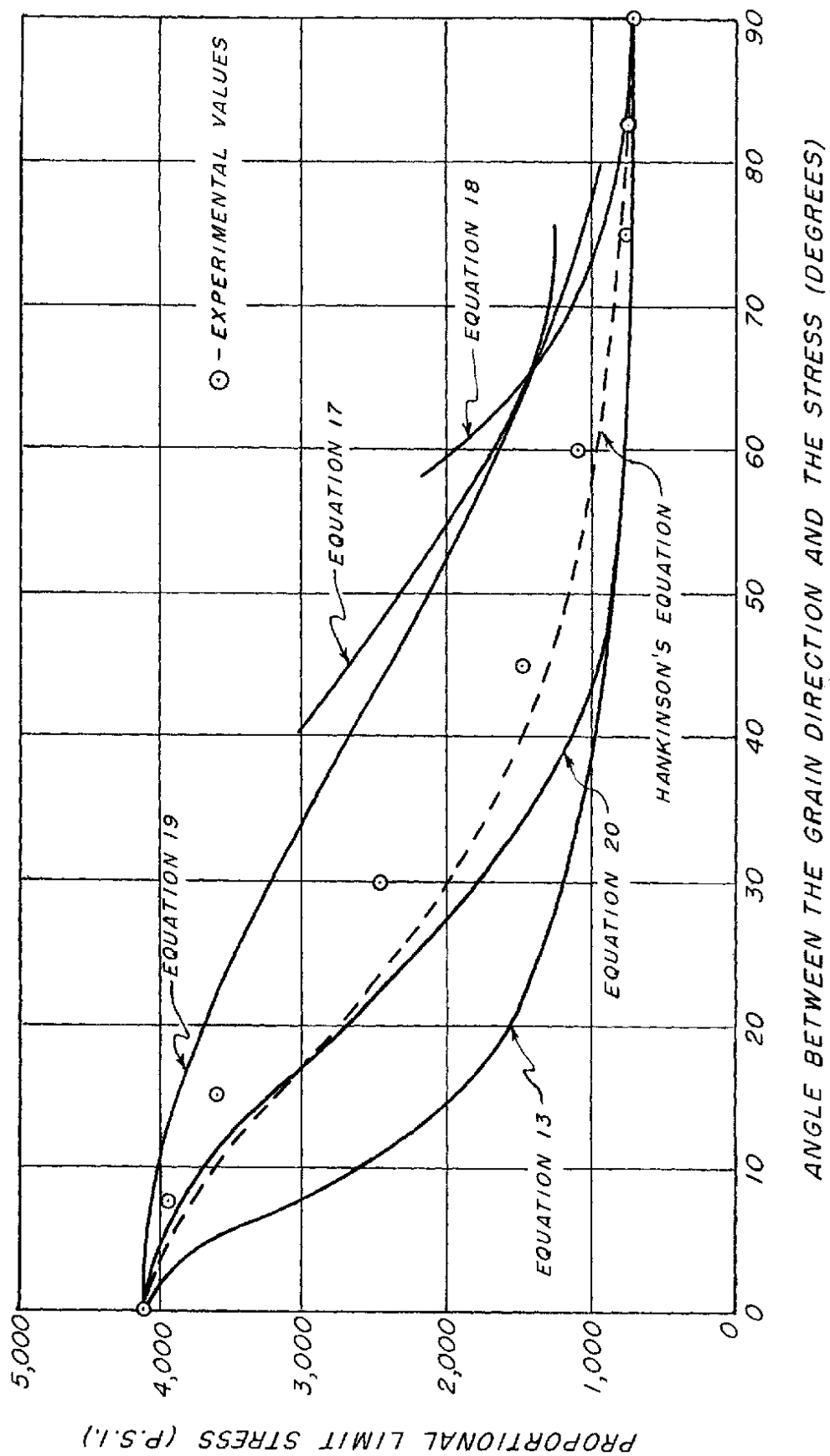


Figure 16. -- Proportionallimit stress in compression of Douglas-fir at various angles to the grain.

SUBJECT LISTS OF PUBLICATIONS ISSUED BY THE  
FOREST PRODUCTS LABORATORY

The following are obtainable free on request from the Director, Forest Products Laboratory, Madison 5, Wisconsin:

List of publications on  
Box and Crate Construction  
and Packaging Data

List of publications on  
Chemistry of Wood and  
Derived Products

List of publications on  
Fungus Defects in Forest  
Products and Decay in Trees

List of publications on  
Glue, Glued Products  
and Veneer

List of publications on  
Growth, Structure, and  
Identification of Wood

List of publications on  
Mechanical Properties and  
Structural Uses of Wood  
and Wood Products

Partial list of publications  
for Architects, Builders,  
Engineers, and Retail  
Lumbermen

List of publications on  
Fire Protection

List of publications on  
Logging, Milling, and  
Utilization of Timber  
Products

List of publications on  
Pulp and Paper

List of publications on  
Seasoning of Wood

List of publications on  
Structural Sandwich, Plastic  
Laminates, and Wood-Base  
Aircraft Components

List of publications on  
Wood Finishing

List of publications on  
Wood Preservation

Partial list of publications  
for Furniture Manufacturers,  
Woodworkers and Teachers of  
Woodshop Practice

Note: Since Forest Products Laboratory publications are so varied in subject no single list is issued. Instead a list is made up for each laboratory division. Twice a year, December 31 and June 30, a list is made up showing new reports for the previous six months. This is the only item sent regularly to the Laboratory's mailing list. Anyone who has asked for and received the proper subject lists and who has had his name placed on the mailing list can keep up to date on Forest Products Laboratory publications. Each subject list carries descriptions of all other subject lists.